

# ELEN4006 - Measurement Systems

## The Design of a Potentiometric-based Smart Transducer for Electric Vehicle Roll Angle Estimation

Jared Ping (704447) & Matthew van Rooyen (706692)

School of Electrical & Information Engineering, University of the Witwatersrand, Private Bag 3, 2050, Johannesburg, South Africa

### Abstract:

**Key words:** Potentiometer, Anti-aliasing Filter, Wheatstone Bridge, Analog-to-Digital Conversion

## 1. INTRODUCTION

Over the last decade, the ever-increasing detrimental effects of CO<sub>2</sub> emissions on the environment has become a much greater problem. This has facilitated a massive growth in the electrification of transportation mediums and, in particular, electric vehicles. With the new technology has come substantial improvements in vehicle and driver active safety control systems.

Vehicle active safety control systems have become increasingly important as a method of reducing the number of motor vehicle accidents on our roads. One such measure is the roll stability control system which automatically responds when a high roll-over risk is detected. This is achieved by controlling the torque applied to the wheels of the vehicle to prevent any uncontrolled handling conditions. The system works by analyzing the angle differential between the wheel base and the road surface. This angle can then be used in order to ascertain when intervention is needed by the control system.

The objective of the project is to investigate the design a potentiometric-based smart transducer in order to calculate the roll angle of a vehicle and the effects the given system will have on the active safety control system. Sensors comprised of potentiometers are often used in accurately measuring angular displacement[? ]. A potentiometer consists of a device placed within resistive coating which makes use of variable resistance to provide a measurable change in potential across the resistive element. The device can be calibrated according to the resistance per unit length which remains constant. The resistance is also directly proportional to this length and thus enables the transducer to convert displacement to resistance.

The proposed solution utilizes a high-bandwidth measurement system in order to accurately measure fast changing parameters of the system. These include instantaneous torque changes, volatile turbulence, and sudden impact. Thus, the measurement system will require a much larger bandwidth than the minimum 100 Hz specified for the design to accurately poll the required system components.

This report documents the design and analysis of the given measurement system. The system static and dynamic characteristics will also be described along with costing and error analysis. Future improvements will also

be suggested.

## 2. PROJECT DETAILS

### 2.1 Success Criteria

The success criteria of the measurement system will be determined by the level of fulfillment of the following specifications:

- A full, critically-analysed design of a smart transducer measurement system has been produced which meets a satisfactory engineering level.
- The system contains all elements set out by Bentley's generalized model of a measurement system.
- The error analysis of a system meets industry standards.
- The design is both energy and cost efficient.
- The system bandwidth exceeds a minimum of 100 Hz.

### 2.2 Assumptions

The following assumptions were made when designing the measurement system:

- It is assumed that there is no limitation on the total cost of the measurement element.
- The operating temperature range is expected to be typical for an electric vehicle.

**2.2.1 Constraints** the following constraints were taken into account when designing the measurement system:

- The system should be designed with a bandwidth of at least 100 Hz.
- 

Regulations??

## 3. SYSTEM DESIGN

### 3.1 Overview

The system was designed according to Bentley's general structure of a measurement system. *Figure 1* shows a block diagram of the system, showing the sensing, signal conditioning, signal processing, and data presentation elements.

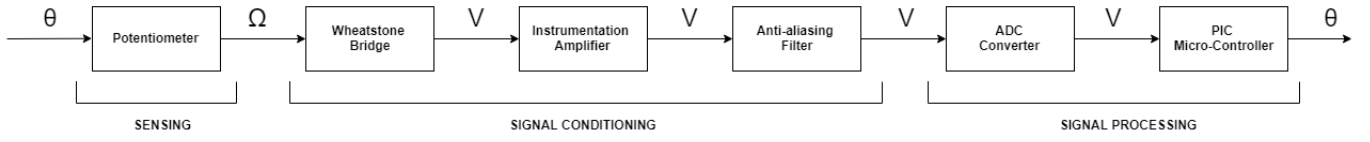


Figure 1: System block diagram, showing the elements of Bentley's general structure of a measurement system

The system takes an input into the system in the form of angular displacement. Using a potentiometer, this then converted to a relative resistance. A Wheatstone bridge makes the conversion from resistance to voltage which is measured in by an instrumentation amplifier. This signal is then filtered to reduce the aliasing error before being sampled by an ADC for processing with a PIC micro-controller. This microprocessor then produces an output which is read into the active safety control system after which decision can be made by the system. Figure 2 indicates the flow diagram representing the interactions of each element.

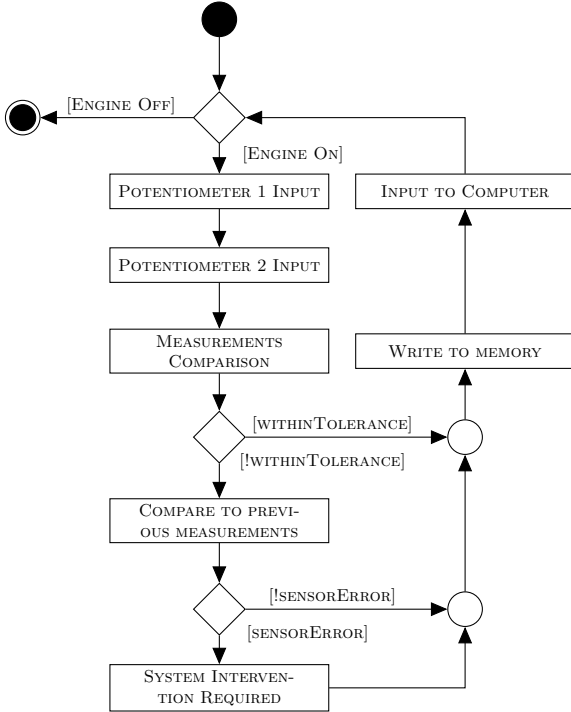


Figure 2: Main measurement processing algorithm

Circuit diagrams for both the Wheatstone bridge and anti-aliasing filter can be found in Appendix. Furthermore, the circuit diagram for the overall measurement design can be found in Appendix of the report.

### 3.2 Sensor

The sensor is responsible for taking the angular displacement and converting it into an electrical signal which can be outputted to the rest of the system. The rotary potentiometer, as shown in fig. 3, contains four primary components: the resistive track, the contact/wiper, the actuator/shaft and the terminations.

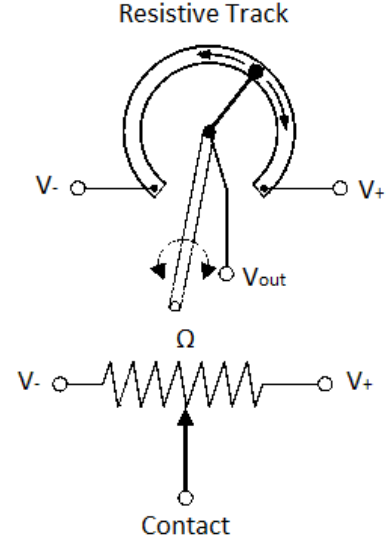


Figure 3: Physical design of a rotary potentiometer

The sensor is connected to the wheel base of the car via the actuator. The actuator is a steel shaft with density  $\rho_{st} = 7850 \text{ kg/m}^3$ , shear modulus  $G_{st} = 79.3 \text{ GPa}$ , and radius 2.6 mm. This shaft is connected directly to the contact which moves along the resistive material providing the drive interface for the sensor. As the angle of elevation of the wheel base varies, a resultant resistance is produced according to the position of the contact along the resistive track. The contact will use a copper multiple-fingered equidistant wiper along the material. This will minimize current crowding along the resistive material reducing the amount of distortion incurred[? ].

The resistive track is made up of a conductive plastic material with a carbon black inert filler. The conductive plastic provides a much more accurate linearity in comparison to other resistive elements such as wirewound or cermet potentiometers due to the method of its manufacturing. It also provides a low contact resistance variation and smoother surface for the contact to move across [? ]. The total length of the resistance band must account for the total range of angular displacement allowed for by the control system. Angular displacement before a critical roll over risk is detected occurs typically between  $-15^\circ$  to  $15^\circ$ . This means that the potentiometer resistance range will occur across a change of  $30^\circ$  respectively with a buffer of  $1^\circ$  to allow for any error or over-extension of the wheel base.

The terminations will be connected to the rest of the cir-

cuit using a solder connection. This provides the advantage of increased reliability and reduces the amount of inductance incurred at the terminations. In addition to this, the solder method provides redundant connection to the resistive track increasing it's ability to handle severe vibrations and therefore increasing it's durability.

**3.2.1 Mechanical Model** A mass-spring-damper model of the potentiometer has been used to find a ratio between the torque and the roll angle output. The conversion between the two states is modeled using a second-order transfer function that considers the friction, spring, damping and inertia experienced by the steel shaft, as shown in *Equation 1*.

$$G(s) = \frac{\theta(s)}{T_{in}(s)} = \frac{1 + \alpha}{Is^2 + Cs + k} \quad (1)$$

where

$$k = \frac{GJ}{l} \quad (2)$$

$$C = \frac{2\pi\mu R^3 l}{d} \quad (3)$$

$$I = \frac{mr^2}{2} \quad (4)$$

$G(s)$  represents the ratio of output angle  $\theta_2(s)$  to input torque  $T_{in}(s)$ .  $k$  represents the steel's elasticity spring constant with  $G$ ,  $J$ ,  $l$  representing the shear modulus, torsional constant, and the length of the shaft respectively.  $C$  is the damping due to the bearings with the value  $\mu$  representing the viscosity of the lubricant supplied for the bearings.  $I$  describes the moment of inertia experienced by the shaft. Using these values, the normalized transfer function is calculated as follows.

$$G_{mech}(s) = \frac{1}{5.605 \times 10^{-8}s^2 + 6.683 \times 10^{-4}s + 1} \quad (5)$$

By analyzing the Bode plot in fig. 4, a limiting mechanical bandwidth of 270 Hz is observed by the circuit.

**3.2.2 Electrical Model** A simple RLC model of a resistor is used to create a transfer function for the electrical component of the potentiometer. A resulting low-pass filter is derived using the lead inductance (10 nH) generated from the terminations as well as the parallel parasitic capacitance (1 pF) contained within the circuit in order to produce the transfer function shown in *Equation 6*.

$$G_{elec}(s) = \frac{1}{1 \times 10^{-20}s^2 + 3 \times 10^{-7}s + 1} \quad (6)$$

### 3.3 Signal Conditioning Element

This process within the system uses the resistance output from the sensor and converts it to a voltage which is

needed for further processing. The following elements are responsible for this process.

**3.3.1 Wheatstone Bridge** The Wheatstone bridge is used to convert the electrical resistance from the potentiometer into a voltage signal. This is achieved by balancing the two legs of the electric circuit containing one unknown resistance. By inputting one variable resistance within the bridge, the voltage range 0V to 5V can be linearized according to the resistance values between  $R_{min}$  to  $R_{max}$ . The resistance values are calculated by balancing the bridge at  $R_{min}$  and linearising the ratios of  $\frac{V_{Th}}{V_s}$  and  $\frac{R(\theta)}{R_{min}}$ . This is achieved by producing a ratio between  $R_3$  and  $R_2$  of 100. The non linearity of the bridge design is calculated as follows:

$$\hat{N} = \frac{V_{Th} - V_{Ideal}}{V_{max}} \cdot 100\% = 2.33\% \quad (7)$$

**3.3.2 Instrumentation Amplifier** The instrumentation amplifier is responsible for converting the voltage difference output of the Wheatstone bridge into a single voltage value.

The amplifier that will be used is the Texas Instruments (TI) INA188. This is a versatile 3 Op-amp precision amplifier with an adjustable gain of between 1 and 1000. The op amp also provides a low input voltage range of approximately 4 V and a high input impedance (100 G $\Omega$  [? ]). For the designed system, the gain will be set to 1 with the amplifier acting as a buffer in order to reduce loading errors incurred by the previous two elements. The bandwidth at this gain is 600 kHz [? ].

**3.3.3 Anti-aliasing Filter** The anti-aliasing (AA) filter is used to reduce the aliasing errors produced when sampling the signal. *Figure 7* in *Appendix A* shows the designed filter. The filter is placed before the Analogue-to-Digital Converter (ADC) in order to eliminate the noise incurred at high-frequency components of the signal and reduce loading effects between the AA filter and the instrumentation amplifier. This is achieved by implementing a second-order low-pass active Butterworth filter with a Salen-Key topology. The Salen-Key topology is chosen due to it's non-inverting gain and it's reduced number of components in comparison to that of a multiple feedback topology. The Butterworth filter is characterized as an active filter providing a smooth pass band and steep roll off as well as a low output impedance.

The filter is designed by using the following equations:

$$Q = \frac{\sqrt{R_1 R_2 C_1 C_2}}{C_2(R_1 + R_2)} = 0.7071 \quad (8)$$

$$f_c = \frac{1}{2\pi\sqrt{R_1 R_2 C_1 C_2}} = 336 \text{ Hz} \quad (9)$$

where  $R_1 = R_2 = 10 \text{ k}\Omega$ . The chosen value of  $Q$  rep-

resents the quality factor at the point where the filter is critically damped.  $f_c$  takes the form of a second-order low pass filter at the -3 dB point frequency.

By substituting in both values, we are able to simultaneously solve for  $C_1$  and  $C_2$ . The closest commercially available values can then be selected for each capacitor. The derived transfer function is calculated in *Equation 10*.

$$G_{AA}(s) = \frac{1}{2.643 \times 10^{-7}s^2 + 1.028 \times 10^{-3}s + 1} \quad (10)$$

The TI LMC6022 operational amplifier will be used as it caters best for the system requirements. The resistors and capacitors used will be 0.1 % and 1 % tolerance respectively in order to reduce the total error experienced by the system.

### 3.4 Signal Processing Element

The signal processing consists of the ADC as well as the microprocessor, a PIC24F08KM101. The ADC is responsible for converting the analogue signal produced by the AA filter into a digital signal which can be read by the PIC.

This PIC has 18 I/O pins, which can all be used as 12 bit ADCs with a 100 kHz sample rate [? ]. It also has 1 MB of RAM as well as a Serial Peripheral Interface (SPI) digital communication module.

The 0.1 % error frequency (-60 dB point) of the AA filter's response is 9.66 kHz, as shown in *Figure 4*. Based on Nyquist's theorem, this means that in order to get an anti-aliasing error of 0.1 %, the signal must be sampled at a minimum of 9.66 kHz. Since this frequency is well below the 100 kHz sample rate of the PIC, there is no need for a separate ADC component in the system.

In addition to ADC functionality, the microprocessor will also be responsible for the storing of angular displacement values in RAM as well as writing them to the data presentation system as discussed in *Section ??*. In order to present the pilot with an angle rather than a voltage, the microprocessor will have a look-up table relating the measured voltages to the appropriate angle. Finally, the microprocessor is responsible for implementing the smart functionality.

The microprocessor will implement a number of smart features. Firstly, it will allow for self calibration by "learning" the maximum and minimum aileron angles on different aircraft. Secondly, the device will be aware of when it was last serviced and will alert the relevant parties when it is due for maintenance. Finally, self diagnosing can be implemented by detecting if one of the two potentiometers on each aileron is not moving while the other is. The relevant party will then be notified and the sensor can be replaced as soon as possible. The dual potentiometer also adds a level of redundancy to the system.

### 3.5 Power Supply

The linearity of the Wheatstone Bridge, discussed in section 3.3.1, is proportional to the magnitude of the DC voltage supplied. Therefore, a trade-off is made such that the DC voltage supplied is reasonably high whilst ensuring the power dissipation is not too large and the cost of the power supply remains affordable. Therefore, in order to satisfy this criteria, Intai IN5100300 51V 300mA switching power supply [? ] is chosen as it meets all the requirements.

## 4. STATIC CHARACTERISTICS

The static characteristics of the system are given in *Table 1*.

Table 1: Characteristics of the measurement system

Static Parameter	Magnitude
Sensor	
Potentiometer input range	$-15^\circ \rightarrow 15^\circ$
Potentiometer output range	$1 \text{ k}\Omega \rightarrow 12 \text{ k}\Omega$
Potentiometer offset	$1 \text{ k}\Omega$
Conductive plastic temp coefficient	$200 \text{ ppm}/^\circ\text{C}$
Bridge output range	$0 \text{ V} \rightarrow 5 \text{ V}$
Bridge maximum power dissipation	$25 \text{ mW}$
INA188	
Gain	1
Gain Drift	$5 \text{ ppm}/^\circ\text{C}$
Offset Voltage	$85 \mu\text{V}$
Input Bias Current	$850 \text{ pA}$
Input Offset current	$850 \text{ pA}$
Operating Temp Range	$-55 \rightarrow 150^\circ\text{C}$
LMC6022	
Input offset voltage	$1 \text{ mV}$
Input offset voltage temp drift	$2.5 \mu\text{V}/^\circ\text{C}$
Input bias current	$0.04 \text{ pA}$
Input offset current	$0.01 \text{ pA}$
Operating temp range	$-40 \rightarrow 85^\circ\text{C}$
System bandwidth	$238 \text{ Hz}$
Step response rise time	$1.5 \text{ ms}$
Step response overshoot	$2.26 \%$
Step response settling time	$3.4 \text{ ms}$

### 4.1 Error Analysis

The information below describes the elements which contribute to the maximum error incurred within the system.

- Accumulative Sensor error: 2.565 %
- Power Supply maximum ripple : 1 %  $V_{p-p}$
- Aliasing error : 0.1 %
- Wheatstone bridge non-linearity :
- Resistor tolerance :  $5 \cdot 0.01 \% = 0.05 \%$
- Capacitor tolerance :  $2 \cdot 1 \% = 2 \%$
- Quantization error : 0.00024 %

The total sensor error is comprised of conductive plastic non-linearity error, potentiometer's contact resistance variation (CRV), bridge maximum non-linearity error. The largest source of error is from the non-linearity of

the bridge, where a total error exceeding 2.5 % is fairly common [? ]. the aim is to reduce this error by increasing the power supply voltage. The error could also be minimised by increasing the load resistance to the largest feasible value.

Resistor and capacitor tolerances for the relevant circuits have been based on typical lower tolerance values for such elements available. While this may increase the price of the device, it is thought to be worth the extra cost to reduce total error of the system.

The total maximum accumulated error of the system is calculated to be 5.74 %.

## 5. DYNAMIC RESPONSE

The bode plot for the system is shown in *Figure 4*. The system transfer function is 6<sup>th</sup> order and is comprised of the transfer functions of the AA filter, the electrical side of the sensor and the mechanical side of the sensor. The bandwidth of the system is 238 Hz. This is clearly a result of the sensor's mechanical side which has a bandwidth of 270 Hz, which is the smallest of the components in the system. The AA filter has a 336 Hz bandwidth, which also impacts the system. The sensor's electrical side has a 528 kHz bandwidth, which is three orders of magnitude larger than the bandwidth system, and has almost no effect on the system's performance. The time domain characteristics are found in *Table 1*.

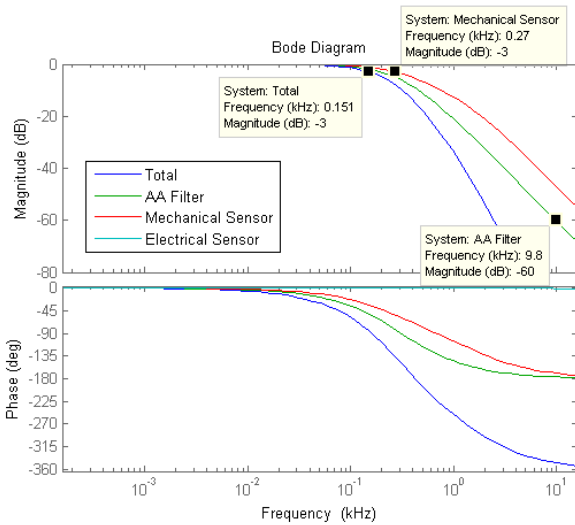


Figure 4: Measurement system Bode plot

## 6. Cost

The estimated cost of the raw materials used to construct the measurement system are shown in *Table 2*. Additional expenses incurred due to the manufacturing process and labour costs were not included in the cost breakdown.

## 7. CONCLUSION

A potentiometric-based smart transducer measurement system is designed for the purpose of measuring an elec-

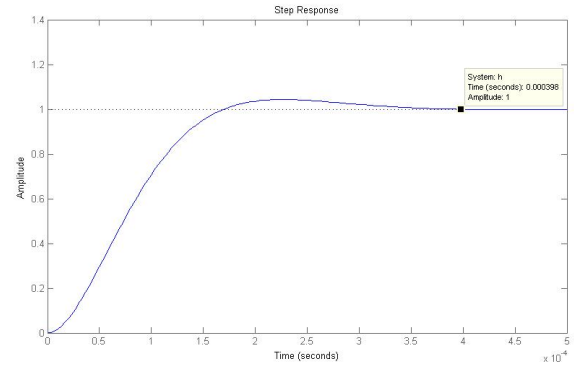


Figure 5: Measurement system step response

Table 2: Component costs for the measurement system

Component	Cost (R)
Conductive Plastic	6.50
Wiper	6.50
Actuator	0.50
IN5100300 (Intai)	189.75
0.1%, 100 $\Omega$ Resistor	92.95
0.1%, 10 k $\Omega$ Resistor $\times 3$	78.65
0.1%, 100 k $\Omega$ Resistor	51.35
1%, 0.082 $\mu$ F Capacitor	29.00
1%, 0.033 $\mu$ F Capacitor	23.40
LMC6022 (TI)	8.00
INA188 (TI)	28.10
PIC24F08KM101	24.30
LS013B4DN04	140.95
<b>Total cost</b>	<b>679.95</b>

tric vehicles roll angle in order to avoid a high roll over risk. A sensor consisting of an angular potentiometer is used to convert the angular displacement measured at the wheel base into a corresponding resistance and finally an electrical current. The current is filtered using an anti-aliasing filter and sampled before being read by an external 12-bit ADC. The information produced by the ADC is then sent to a microcontroller where the information is stored before being transferred to a computer which communicates with the active safety control system already in place in the vehicle. The maximum output error of the measurement system is approximately %. The static and dynamic characteristics of the system have been critically analyzed and detailed in this report. The total cost of the measurement system is R679.95.

## Appendix

### A Circuit Diagrams

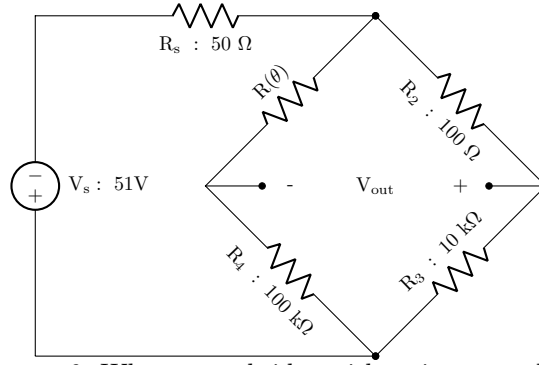


Figure 6: Wheatstone bridge with resistance values

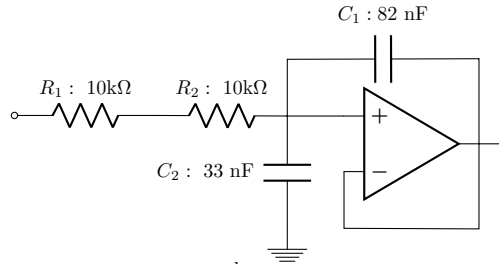


Figure 7: 2<sup>nd</sup> order AA filter.

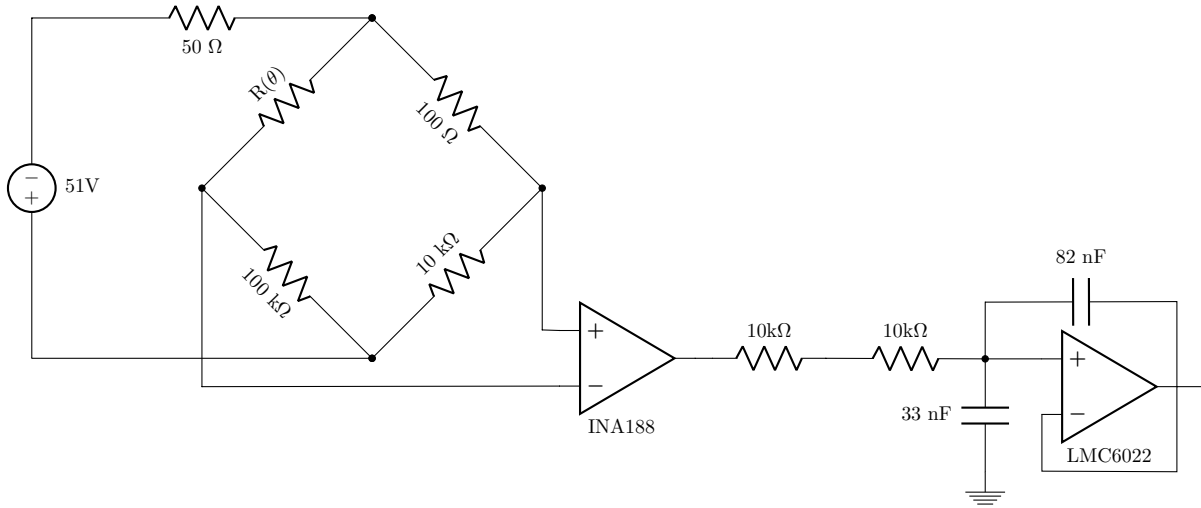


Figure 8: Total circuit diagram